Quantitative apical membrane proteomics reveals vasopressin-induced actin dynamics in collecting duct cells

Chin-San Loo[a,1], Cheng-Wei Chen[a,1], Po-Jen Wang[a], Pei-Yu Chen[a], Shu-Yu Lin[b], Kay-Hooi Khoo[b], Robert A. Fenton[c], Mark A. Knepper[d], and Ming-Jiun Yu[a,2]

[a]Institute of Biochemistry and Molecular Biology, National Taiwan University College of Medicine, Taipei 10051, Taiwan; [b]Institute of Biological Chemistry, Academia Sinica, Taipei 11529, Taiwan; [c]Department of Biomedicine, InterPrET Center, Aarhus University, Aarhus 8000, Denmark; and [d]Systems Biology Center, National Heart, Lung, and Blood Institute, Bethesda, MD 20892

Edited by Maurice B. Burg, National Heart, Lung, and Blood Institute, Bethesda, MD, and approved September 5, 2013 (received for review May 20, 2013)

In kidney collecting duct cells, filamentous actin (F-actin) depolymerization is a critical step in vasopressin-induced trafficking of aquaporin-2 to the apical plasma membrane. However, the molecular components of this response are largely unknown. Using stable isotope-based quantitative protein mass spectrometry and surface biotinylation, we identified 100 proteins that showed significant abundance changes in the apical plasma membrane of mouse cortical collecting duct cells in response to vasopressin. Fourteen of these proteins are involved in actin cytoskeleton regulation, including actin itself, 10 actin-associated proteins, and 3 regulatory proteins. Identified were two integral membrane proteins (Clmn, Nckap1) and one actin-binding protein (Mpp5) that link F-actin to the plasma membrane, five F-actin end-binding proteins (Arpc2, Arpc4, Gsn, Scin, and Capzb) involved in F-actin reorganization, and two actin adaptor proteins (Dbn1, Lasp1) that regulate actin cytoskeleton organization. There were also protease (Capn1), protein kinase (Cdc42bpb), and Rho guanine nucleotide exchange factor 2 (Arhgef2) that mediate signal-induced F-actin changes. Based on these findings, we devised a live-cell imaging method to observe vasopressin-induced F-actin dynamics in polarized mouse cortical collecting duct cells. In response to vasopressin, F-actin gradually disappeared near the center of the apical plasma membrane while consolidating laterally near the tight junction. This F-actin peripheralization was blocked by calcium ion chelation. Vasopressin-induced apical aquaporin-2 trafficking and forskolin-induced water permeability increase were blocked by F-actin disruption. In conclusion, we identified a vasopressin-regulated actin network potentially responsible for vasopressin-induced apical F-actin dynamics that could explain regulation of apical aquaporin-2 trafficking and water permeability increase.

SILAC | LC-MS/MS | proteome | dDAVP | AQP2

Vasopressin regulates aquaporin-2 (AQP2) and osmotic water transport in the collecting duct by regulating total AQP2 protein abundance and AQP2 trafficking to and from the apical plasma membrane of principal cells (1). Understanding these regulatory mechanisms at the molecular level is important to the ultimate understanding of the pathophysiology of multiple water balance disorders (2). This goal is abetted by the methods of molecular systems biology (proteomics and transcriptomics), which not only reveal "parts lists" for collecting duct cells but also can identify what biological and molecular processes are regulated by vasopressin. These proteomic and transcriptomic data have been made publicly available in databases (3). Many of these studies have focused on whole cells (4–6), whereas several analyzed subcellular fractions (7–12). Analysis of subcellular fractions is technically demanding, but it has the benefit of identifying low abundance proteins with important functions. To identify proteins potentially involved in apical AQP2 trafficking, we previously used NHS-based surface biotinylation coupled to streptavidin-affinity chromatography to enrich apical plasma membrane proteins of native rat kidney collecting ducts and identified these proteins by mass spectrometry (MS) (12). A number of apical membrane proteins involved in vesicular trafficking and cytoskeletal regulation were identified. However, several technical barriers prohibited deeper quantitative analysis: (*i*) labeling of the apical plasma membrane of native collecting ducts required technically difficult perfusion of the biotinylation reagent into the collecting duct lumens; (*ii*) AQP2, the major vasopressin target, was not efficiently biotinylated because it has only one extracellular NHS-reactive lysine that is likely occluded by an adjacent N-glycosylation site in the second extracellular loop; and (*iii*) investigation of native collecting ducts precluded the use of in vivo metabolic labeling for accurate quantification of protein abundance changes. In this study, we overcame these limitations by using stable-isotope labeling with amino acids in cell culture (SILAC) methodology in cultured mouse cortical collecting duct (mpkCCD-clone 11) cells (4) that had undergone apical surface biotinylation with a reagent that targets extracellular *N*-glycosyl groups (13). Biotinylated proteins were identified

Significance

Vasopressin is a peptide hormone that regulates renal water excretion to maintain whole-body water balance. It does so by regulating trafficking of a molecular water channel, aquaporin-2, to and from the plasma membrane of collecting duct cells. This study uses two state-of-the-art methods (protein mass spectrometry of affinity-isolated apical plasma membrane proteins and live-cell imaging of actin dynamics) to uncover the central role of the actin dynamics in the trafficking of aquaporin-2–containing vesicles. The results coupled with prior data produce a model in which vasopressin signaling triggers actin accumulation near the tight junction and concomitant depletion of actin from the central regions of the apical plasma membrane, thereby providing access of aquaporin-2–containing vesicles to the apical plasma membrane.

Author contributions: C.-S.L., C.-W.C., P.-J.W., P.-Y.C., R.A.F., and M.-J.Y. designed research; C.-S.L., C.-W.C., P.-J.W., P.-Y.C., S.-Y.L., K.-H.K., R.A.F., and M.-J.Y. performed research; C.-S.L., C.-W.C., P.-J.W., P.-Y.C., S.-Y.L., K.-H.K., R.A.F., M.A.K., and M.-J.Y. analyzed data; and C.-S.L., C.-W.C., R.A.F., M.A.K., and M.-J.Y. wrote the paper.

The authors declare no conflict of interest.

This article is a PNAS Direct Submission.

Data deposition: The proteomic results reported in this paper have been deposited in the mpkCCD Quantitative Apical Membrane Proteome database, http://sbel.mc.ntu.edu.tw/mpkCCDqAMP/qAMP.htm. The mass spectrometry proteomics data reported in this paper have been deposited in the ProteomeXchange Consortium, http://proteomecentral.proteomexchange.org, via the PRoteomics IDEntifications Database (PRIDE) partner repository (dataset identifier PXD000399).

[1]C.-S.L. and C.-W.C. contributed equally to this work.

[2]To whom correspondence should be addressed. E-mail: mjyu@ntu.edu.tw.

This article contains supporting information online at www.pnas.org/lookup/suppl/doi:10.1073/pnas.1309219110/-/DCSupplemental.

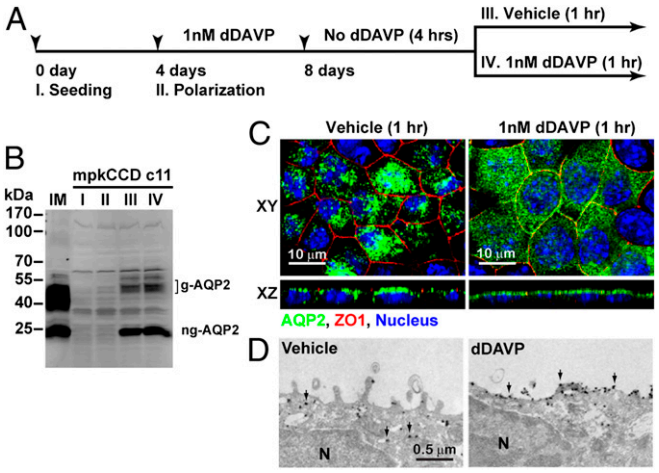

Fig. 1. Induction of endogenous AQP2 expression and apical trafficking in mpkCCD clone 11 cells using dDAVP. (*A*) Experimental protocol. (*B*) Immunoblotting for AQP2 levels at various stages in the experimental protocol. g-AQP2, glycosylated AQP2; I, II, III, and IV, protein samples collected at various experimental stages as in *A*; IM, mouse kidney inner medulla lysate; ng-AQP2, nonglycosylated AQP2. (*C*) Confocal immunofluorescence staining of AQP2. ZO1, zonula occludens protein 1. (*D*) Immunoelectron microscopic staining of AQP2. Arrow, AQP2; N, nucleus.

and quantified by liquid chromatography–tandem MS (LC-MS/MS) to discover vasopressin-regulated apical membrane proteins. Consistent with the principles of systems biology (1), the objective was not to identify novel individual proteins but, rather, to identify biological processes involved in regulation of AQP2 trafficking. Of the identified biological processes, regulation of actin filament polymerization was an area previously thought to be involved in AQP2 trafficking and was, thus, subsequently followed up using hypothesis driven approaches.

Results

The mpkCCD Cell Model for Vasopressin-Induced Apical AQP2 Trafficking. Before using the mpkCCD cells, we first confirmed vasopressin-induced regulation of AQP2. Fig. 1*A* illustrates the experimental protocol. Fig. 1*B* shows an immunoblot probed for AQP2. Nonpolarized and polarized mpkCCD cells not treated with the vasopressin analog 1-deamino-8-D-arginine vasopressin (dDAVP) did not express detectable levels of AQP2 protein (Fig. 1*B*, lanes I and II). Addition of dDAVP to the basolateral medium of polarized cells induced AQP2 protein expression (Fig. 1*B*, lanes III and IV). Withdrawal of dDAVP for 4 h followed by reapplication of vehicle or dDAVP to the basolateral medium for 1 h did not alter overall AQP2 protein levels (Fig. 1*B*, lanes III vs. IV). However, reapplication of dDAVP induced AQP2 redistribution from intracellular vesicles to the apical plasma membrane as seen by immunofluorescence confocal microscopy (Fig. 1*C*) and immunogold electron microscopy (Fig. 1*D*). Thus, the mpkCCD cells recapitulated vasopressin-induced AQP2 abundance increases and apical trafficking as seen in native kidney collecting duct principal cells. Note that both glycosylated AQP2 and nonglycosylated AQP2 were observed on immunoblots (Fig. 1*B*).

Quantitative Analysis of the Apical Plasma Membrane Proteome in Response to Vasopressin. Apical membrane proteins of the mpkCCD cells were biotinylated with biocytin hydrazide, which reacts with oxidized glycans of glycosylated proteins, allowing isolation for MS analysis. As seen in Fig. 2*A*, sites of biotinylation were restricted to the apical membrane of the mpkCCD cells regardless of the absence or presence of dDAVP. In the absence of dDAVP, AQP2 was present largely in intracellular vesicles and did not colocalize with biotin (Fig. 2*A*, *Upper*). In the presence of dDAVP, AQP2 trafficked to the apical membrane where it colocalized with the biotin label (Fig. 2*A*, *Lower*). The biotinylated apical membrane proteins from either vehicle or dDAVP treated cells were concentrated in the eluate (i.e., apical membrane) fraction using streptavidin-affinity chromatography (Fig. 2*B*, *Upper*). AQP2 protein abundance was increased in the eluate of the cells treated with dDAVP vs. vehicle (Fig. 2*B*, *Lower*, lane E).

Apical membrane proteins from stable isotope-labeled mpkCCD cells treated with vehicle or dDAVP were collected for quantitative MS analysis (Fig. S1). Three independent replicates were analyzed (Fig. S2). dDAVP-treated cells were alternated between heavy- and light-isotopic labels (Fig. S2*A*). The expectation is that apical-surface biotinylation will retrieve not only integral membrane proteins (IMPs) but also peripheral membrane proteins bound to them, as previously observed (12). Fig. 2 *C* and *D* summarize the results from three experiments. Compared with the vehicle control, dDAVP significantly increased the amount of apical AQP2, regardless of isotope labeling. A total of 2,093 proteins were quantified in three experiments (Fig. 2*D*). Among them, 1,028 proteins were quantified in all three experiments. A volcano plot summarizes all 1,028 quantified proteins (Fig. 3*A*), of which 100 proteins showed significant ($P < 0.05$) abundance changes in the apical membrane of mpkCCD cells in response to dDAVP (Tables S1 and S2), and 5 of these (including 4 IMPs) had values of $\log_2$ (dDAVP/vehicle) > 0.5. AQP2 showed the greatest abundance increase in the apical membrane in response to dDAVP, followed by protein Mal2 (Mal2) (a lipid raft protein involved in transcytosis), calmin isoform b (Clmn) (a calponin-like actin binding protein), and membrane-associated guanylate kinase p55 subfamily member 5 (Mpp5) (a PDZ- and SH3-domain–containing scaffold protein involved in tight junction biogenesis and actin dynamics). Tumor necrosis factor receptor superfamily member 10B (Tnfrsf10b), a cytotoxic ligand receptor that is essential for endoplasmic reticulum stress-induced apoptosis, showed the greatest decrease in apical abundance. Immunoblotting and confocal immunofluorescence microscopy confirmed the increases in the amount of AQP2 and Mal2 in the apical plasma membrane in

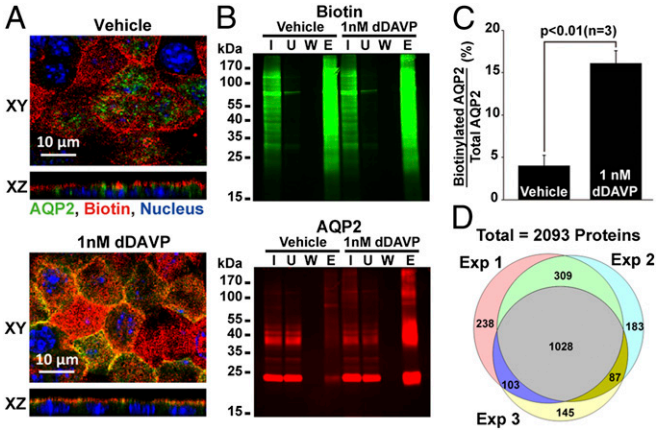

Fig. 2. Quantitative analysis of apical membrane proteome of mpkCCD cells in response to dDAVP. (*A*) Fluorescence staining of sites of biotinylation and AQP2 in the mpkCCD cells. Vehicle- and dDAVP-treated mpkCCD cells were subjected to apical surface biotinylation using biocytin hydrazide. Sites of biotinylation and AQP2 were visualized with Alexa568-conjugated streptavidin and AQP2 specific antibody, respectively. (*B*) Gel image of biotinylated proteins and immunoblotting of AQP2. Apical membrane proteins of vehicle- and dDAVP-treated mpkCCD cells were biotinylated and purified with streptavidin-affinity chromatography before analysis for biotin labeling and AQP2. E, eluate; I, input cell lysate; U, unbound fraction; W, fifth wash solution. (*C*) A summary of three AQP2 immunoblotting results as described in *B*. (*D*) Venn diagram summary of proteins quantified in three SILAC-based apical membrane proteomics experiments.

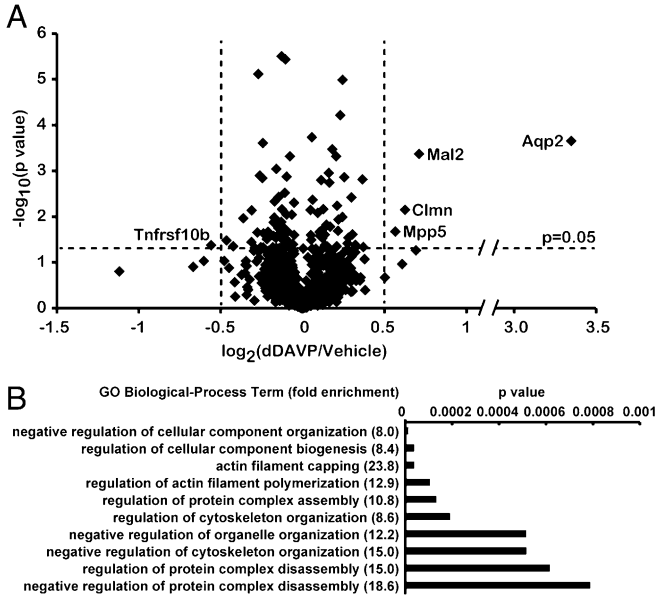

Fig. 3. Bioinformatic analysis of dDAVP-regulated apical membrane proteins. (*A*) Volcano plot summary of SILAC-based quantification of 1,028 apical plasma membrane proteins ($n = 3$). Log_2(dDAVP/vehicle), base 2 logarithmic value of protein abundance ratio (dDAVP vs. vehicle). Log_{10}(*P* value), base 10 logarithmic value of *P* value of *t* test, log_2(dDAVP/vehicle) vs. log_2 (1). (*B*) GO Biological Process terms extracted for the 100 dDAVP-regulated proteins. The *P* values were obtained using Fisher's exact test against all transcripts expressed in mpkCCD cells (4).

response to dDAVP (Figs. 2 *A* and *B* and 4). A list of all quantified proteins can be accessed at http://sbel.mc.ntu.edu.tw/mpkCCDqAMP/qAMP.htm.

To transform the list of 100 dDAVP-regulated apical membrane proteins to a list of biological processes regulated by dDAVP, we extracted Gene Ontology (GO) Biological Process terms. Among the Biological Process terms significantly ($P < 0.01$) enriched were "negative regulation of cellular component organization," "actin filament capping," "regulation of actin filament polymerization," and "regulation of cytoskeleton organization," compared with all transcripts in the mpkCCD cells (Fig. 3*B*). In contrast to the dDAVP-regulated proteins, the 928 apical membrane proteins not regulated by dDAVP yielded a much different list of significantly ($P < 0.01$) enriched GO Biological Process terms: "cellular carbohydrate catabolic process," "cellular amino acid and derivative metabolic process," "oxidation reduction," etc. (Fig. S3). This comparison is compatible with the existing view (*Discussion*) that vasopressin regulates the actin cytoskeleton adjacent to the apical membrane of collecting duct cells. Fig. 5 summarizes 14 dDAVP-regulated apical membrane proteins involved in actin cytoskeleton organization, including actin itself, 10 actin-binding proteins, and 3 actin-regulatory proteins. Clmn and nck-associated protein 1 (Nckap1) (14) are actin binding IMPs. Actin-related protein 2/3 complex subunit 2/4 (Arpc2 and Arpc4) (15), gelsolin isoform 2 (Gsn) (16), adseverin isoform-1 (Scin) (17–19), and filamentous actin (F-actin) capping protein β (Capzb) (20) are F-actin end-binding proteins. Mpp5 (21, 22), drebrin-like protein isoform 3 (Dbn1) (23–25), and LIM and SH3 domain protein 1 (Lasp1) (26) are actin-binding adaptor proteins. Calpain-1 catalytic subunit (Capn1) is a protease (27, 28). Serine/threonine-protein kinase MRCK β (Cdc42bpb) (29) and Rho guanine nucleotide exchange factor 2 (Arhgef2) (30) are actin-regulatory proteins.

Apical F-Actin Dynamics in mpkCCD Cells Induced by dDAVP. To evaluate roles of F-actin in vasopressin-mediated apical AQP2 trafficking, we devised a live-cell imaging method to observe F-actin in the apical membrane region of mpkCCD cells in response to dDAVP (Fig. S4). In response to dDAVP, the F-actin near the center of the apical membrane disappeared over 25 min, while it became concentrated laterally near the tight junctions (Fig. 6*A* and Movie S1). Under control conditions, F-actin was seen to form and deform in a cyclic manner in the apical membrane region (Fig. 6*B* and Movie S2). Fluorescence staining using rhodamine-conjugated phalloidin confirmed that dDAVP reduced apical F-actin abundance (Fig. 6*C*).

Calcium-Dependent Apical F-Actin Redistribution Induced by dDAVP. To investigate the role of calcium in vasopressin-induced F-actin dynamics and apical AQP2 trafficking, BAPTA-AM (1,2-Bis(2-aminophenoxy)ethane-N,N,N′,N′-tetraacetic acid tetrakis(acetoxymethyl ester)) was used to chelate intracellular calcium. With the vehicle (DMSO) pretreatment, dDAVP induced F-actin peripheralization in the apical membrane region (Fig. 6*D* and Movie S3). When intracellular calcium was buffered with BAPTA-AM, the dDAVP-induced F-actin redistribution was abolished (Fig. 6*E* and Movie S4). In addition, BAPTA-AM also blocked dDAVP-induced apical AQP2 localization (Fig. 7*D*), whereas the vehicle control had no effects on dDAVP-induced apical AQP2 localization (Fig. 7*B*).

F-Actin Integrity Required for dDAVP-Induced Apical AQP2 Trafficking and Forskolin-Induced Water Permeability Increase. To investigate roles of dDAVP-induced F-actin dynamics in apical AQP2 trafficking, latrunculin B was used to inhibit F-actin polymerization. Latrunculin B alone disrupted F-actin in the mpkCCD cells, whereas the vehicle (DMSO) did not (Fig. 7 *A* and *E*). When F-actin was disrupted with latrunculin B, dDAVP-induced apical AQP2 localization was disrupted (Fig. 7*F*) and so was forskolin-induced water permeability increase (Fig. S5 and Table S3), consistent with the prior finding that latrunculin B inhibits vasopressin induced osmotic water permeability increases in isolated perfused rat collecting ducts (31). The vehicle control (DMSO) did not affect dDAVP-induced apical AQP2 localization (Fig. 7*B*) or forskolin-induced water permeability increase (Table S3).

Discussion

After the initial recognition of the roles of cytoskeletal elements in the hydroosmotic response to vasopressin (32), the involvement of vasopressin-induced F-actin depolymerization in the apical cell cortex was demonstrated by Hays and coworkers in toad bladder epithelial cells (33, 34) and in rat inner medullary collecting duct cells (35). The apical F-actin network was thought to function as a barrier that blocks access of AQP2-containing vesicles to the apical plasma membrane in the absence of vasopressin. In this model, vasopressin-induced local depolymerization of apical F-actin allows access of AQP2-containing vesicles to the apical plasma membrane, facilitating vesicle docking and fusion, thereby increasing the water permeability of the membrane. Multiple additional studies provided strong support for roles of F-actin depolymerization in vasopressin-induced apical AQP2 trafficking

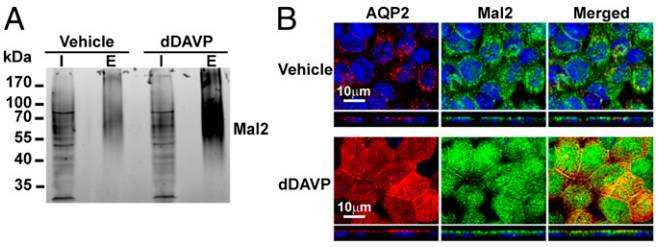

Fig. 4. Mal2 response to dDAVP. (*A*) Surface biotinylated apical membrane proteins of vehicle- and dDAVP-treated mpkCCD cells were purified and immunoblotted for Mal2. (*B*) Immunofluorescence localization of Mal2 and AQP2 in vehicle- and dDAVP-treated mpkCCD cells. E, eluate; I, input cell lysate.

PHYSIOLOGY

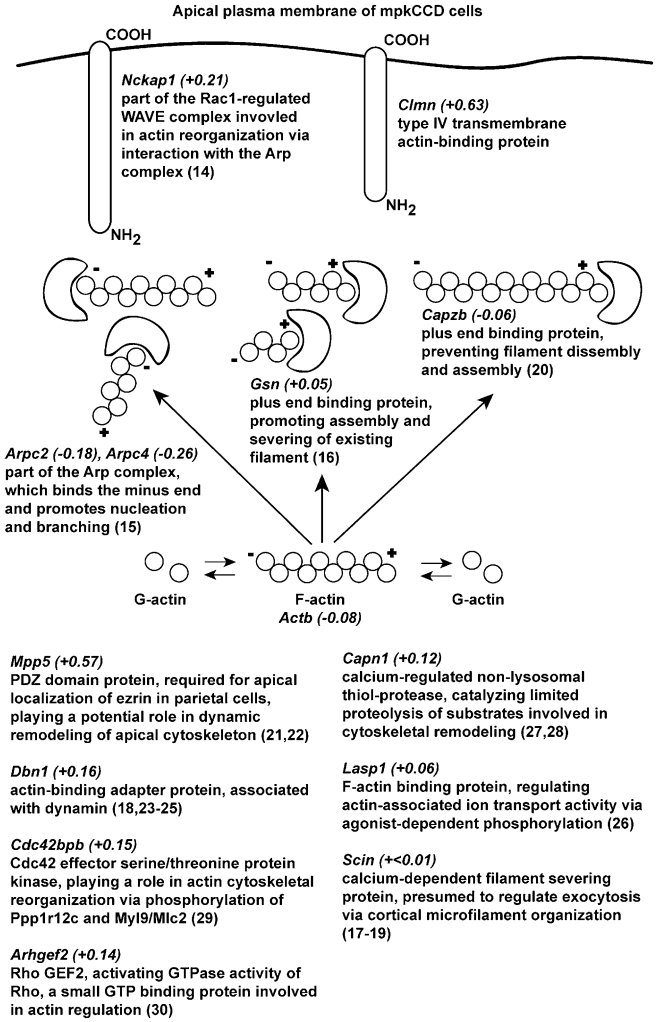

Fig. 5. dDAVP-regulated apical membrane proteins involved in actin cytoskeleton regulation. Official gene symbols for each protein are shown with their abundance changes expressed as $\log_2$(dDAVP/vehicle) in parentheses.

(31, 36–43). Furthermore, inhibition of Rho, a small GTPase protein involved in actin polymerization (44), results in AQP2 membrane localization (36, 38, 42, 45). Activation of Rho by bradykinin, a peptide hormone that reduces vasopressin-induced water permeability in isolated, perfused collecting ducts (46), promotes actin polymerization, and inhibits apical AQP2 localization (47). These observations support an "actin-driven transport" model for apical AQP2 trafficking (48). Recently AQP2 was shown to "catalyze" F-actin depolymerization, thus taking an active role in its own trafficking (37). Until now, direct observation of vasopressin-induced dynamic changes of apical F-actin has not been visualized in live, polarized collecting duct cells that express endogenous AQP2, and the molecular components involved have been largely missing.

The mpkCCD cells used in this study were originally developed by Vandewalle and coworkers (49) and were recloned (clone 11) to select for maximum endogenous vasopressin-inducible AQP2 expression levels (4). Using the latter, we confirmed that the cells respond to dDAVP with induction of AQP2 gene expression, apical trafficking (Fig. 1), and increased water permeability (Table S3), observations consistent with those in native collecting duct cells (50). Thus, we conclude that the mpkCCD-clone 11 cell line is an appropriate model for systems approaches to understanding AQP2 regulation, because it likely hosts all necessary molecular components of vasopressin signaling required for regulation of AQP2 gene expression and trafficking. Furthermore, the availability of a number of transcriptome and proteome databases of this mpkCCD-clone 11 cell line provides the necessary informational infrastructure for systems level studies of vasopressin-mediated AQP2 regulation (4, 9, 51, 52).

To identify proteins involved in vasopressin-regulated apical membrane trafficking, we chose glycan-reactive biocytin hydrazide to label apical membrane proteins because primary amine-reactive NHS-based biotinylation agents yielded very low labeling efficiency of AQP2 in the mpkCCD-clone 11 cells and in native rat collecting duct cells (12). One possible explanation is that protein glycosylation may occlude access of the NHS-based biotinylation reagent to the only extracellular lysine of AQP2, found on the second extracellular loop (C-loop). Endogenous AQP2 in native kidney collecting duct cells and in mpkCCD-clone 11 cells is highly glycosylated (4, 12) via N-linked glycosylation at an asparagine residue also in the C-loop of AQP2 (53). It seems plausible that NHS-based biotinylation has succeeded in cells in which AQP2 is ectopically expressed (54) because the extent of glycosylation is less (either smaller glycosyl trees or fewer subunits of the AQP2 tetramer glycosylated), therefore affording greater access of the reagent to the C-loop lysine.

Using biocytin hydrazide and streptavidin-affinity chromatography, we quantified changes in the apical abundance of 2,093 proteins in mpkCCD-clone 11 cells in response to dDAVP (Fig. 2) based on state-of-the-art methods [i.e., stable-isotope labeling (SILAC) and LC-MS/MS]. Our method allowed identification of integral membrane proteins, as well as peripheral membrane proteins bound to them, because the mild detergent combination preserved protein–protein interactions (12). Among the 2,093 quantified proteins, 100 showed significant apical abundance changes. Of the 100 proteins, 22 integral membrane proteins plus 1 GPI-anchored protein constituted the largest protein group (Tables S1 and S2). The second largest protein group is 14 proteins

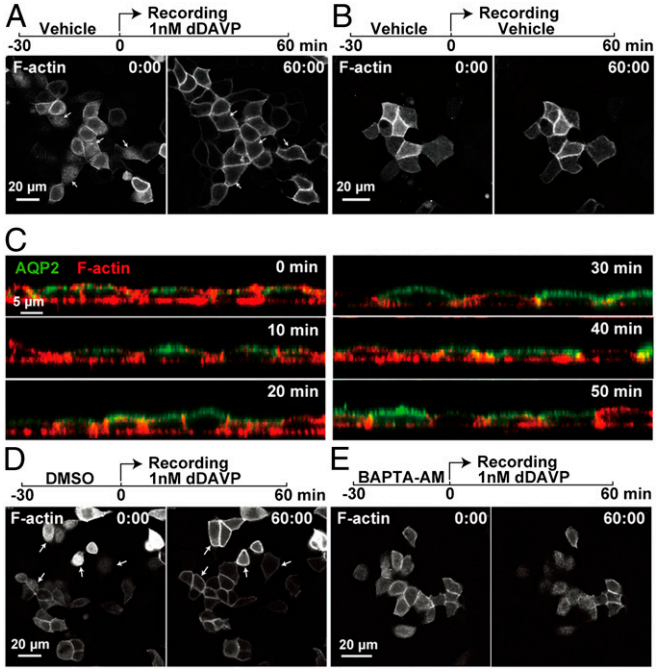

Fig. 6. Vasopressin-induced calcium-dependent apical F-actin dynamics in mpkCCD cells. First (00 min:00 s) and last (60 min:00 s) images from recordings of apical F-actin in live and polarized mpkCCD cells in the presence (*A*) or absence (*B*) of dDAVP. (*C*) Time course of AQP2 and F-actin localization changes in mpkCCD cells following dDAVP treatment. First (00 min:00 s) and last (60 min:00 s) images from recordings of apical F-actin in mpkCCD cells pretreated with vehicle (DMSO) (*D*) or 50 μM BAPTA-AM intracellular calcium chelator (*E*) before the cells were exposed to dDAVP.

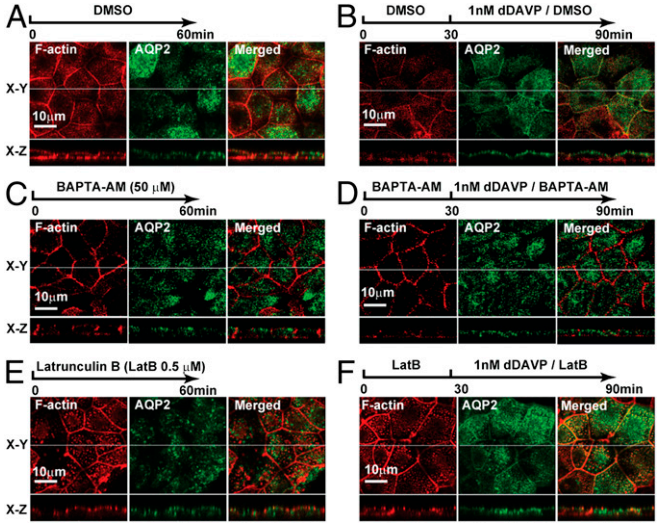

Fig. 7. F-actin–dependent vasopressin-induced apical AQP2 localization. (*A* and *B*) Localization of AQP2 and F-actin in mpkCCD cells in the absence (DMSO) or presence of dDAVP. (*C* and *D*) Localization of AQP2 and F-actin in mpkCCD cells in the presence of BAPTA-AM (50 μM) without or with dDAVP. (*E* and *F*) Localization of AQP2 and F-actin in mpkCCD cells in the presence of latrunculin B (0.5 μM) without or with dDAVP.

involved in regulation of the actin cytoskeleton (Fig. 5). These proteins include actin (Actb), accessory proteins that bind and affect F-actin structures and regulatory proteins that mediate extracellular signal-induced F-actin changes. In an earlier study, immunoisolation of AQP2 from rat kidney followed by MALDI-TOF identification of coisolated proteins also identified a number of actin-related proteins [i.e., actin itself, myosin regulatory light chain, a tropomyosin isoform, scinderin, gelsolin, α-actinin 4, α-II spectrin, and nonmuscle myosin II-A (18)]. The results of these two proteomics studies, therefore, are compatible with the idea that the actin cytoskeleton indeed plays a role in the regulation of AQP2 trafficking and, together, provided us with the impetus to look for evidence of a dynamic response of F-actin to vasopressin using live-cell imaging of F-actin. These dynamic imaging studies demonstrated that vasopressin induces a distinct pattern of F-actin depolymerization, with loss of F-actin in the apical cell pole near the center of the cell and concomitant dense accumulation of F-actin laterally in the vicinity of the tight junctions (Fig. 6 *A*, *C*, and *D* and Movies S1 and S3).

Several mechanisms may explain F-actin peripheralization induced by vasopressin. Vasopressin may induce local F-actin depolymerization near the center of the cells with concomitant F-actin polymerization close to the tight junctions. Whereas the former could result from Rho inhibition near the center of the cells after vasopressin stimulation (38, 42), the latter would require Rho activation at the tight junctions (i.e., differential regulation of Rho activity at the cell center vs. cell periphery by vasopressin). Another possible mechanism is asymmetrical actomyosin tensions at the cell center vs. cell periphery. The actomyosin tension is a force generated via interaction between F-actin and the actin-based molecular motor [i.e., nonmuscle myosin II (55)]. Either a decrease in the central actomyosin tension and/or an increase in the peripheral tension could result in F-actin peripheralization. Local actomyosin relaxation seems possible in view of the fact that vasopressin was shown to relax cortical actomyosin interactions in primary rat inner medullary collecting cells (39). As the actomyosin tension relaxes in the cell center, the remaining peripheral tension can be expected to pull F-actin toward the cell periphery. An increase in the peripheral actomyosin tension is also a possibility because vasopressin has been shown to activate myosin light chain kinase (31), which, in turn, activates myosin light chain and hence nonmuscle myosin II activity (55). In the ear's organ of Corti, the nonmuscle myosin IIB and IIC, not IIA, are organized as a sarcomeric network surrounding the apical perimeter of the cells (56). This arrangement was shown to regulate the length of the apical perimeter and the apical surface area. It would be of interest to examine cellular localization of various nonmuscle myosin II proteins in native and mpkCCD-clone 11 collecting duct cells. Regardless of the mechanism, vasopressin-induced F-actin peripheralization is expected to yield a pathway for AQP2-containing vesicles to move toward, and subsequently dock and fuse with, the apical plasma membrane.

Mal2 showed the second greatest increase in apical abundance in mpkCCD-clone 11 cells in response to dDAVP (Fig. 3). Mal2 is a protein with four membrane-spanning helices that is involved in trafficking of apical membrane proteins via transcytosis (57), in which the apical membrane proteins are first delivered to the basolateral membrane before they are endocytosed and targeted to the apical membrane. AQP2 has been reported in the basolateral membrane in native collecting duct cells and cultured epithelial cells (58, 59). It is possible that Mal2 may be involved in vasopressin-induced apical AQP2 trafficking via the transcytosis mechanism (59).

In summary, using modern quantitative proteomics, we identified a number of vasopressin-regulated F-actin regulatory proteins in the apical plasma membrane of mpkCCD-clone 11 cells. Using live-cell imaging in polarized mpkCCD-clone 11 cells, we observed vasopressin-induced Ca^{2+}-dependent apical F-actin dynamic changes that participate in vasopressin-induced apical trafficking of AQP2 and water permeability increase.

Materials and Methods

Cell Culture. Mouse kidney collecting duct cells, mpkCCD-clone 11 (4), were grown on membrane supports until polarized before experiments. Culture procedures are described in *SI Materials and Methods*.

Immunoblotting, Immunofluorescence, and Immunoelectron Microscopy. Immunoblotting and immunofluorescence confocal microscopy were carried out as described previously (12) with modifications. For immunoelectron microscopy, cells grown on membrane supports were fixed with paraformaldehyde and stained with primary antibody and gold-labeled secondary antibody. After poststaining fixation with glutaraldehyde, silver enhancement was performed to increase visibility of the gold particles.

Apical Membrane Protein Labeling. Biocytin hydrazide was used to label apical membrane proteins following the method of Tamma et al. (13) with modifications. Briefly, the apical plasma membrane of the cells were treated with sodium periodate, which oxidizes the glycan of the apical membrane proteins before biocytin hydrazide labeling. Labeled apical membrane proteins were purified with streptavidin-affinity chromatography (12).

Quantitative Protein Mass Spectrometry. SILAC was coupled to LC-MS/MS for quantitative analysis of the mpkCCD apical membrane proteome in response to dDAVP (51). Cell proteins were metabolically labeled with light or heavy amino acids before experimental treatments, corresponding to vehicle vs. dDAVP or vice versa. Vehicle- and dDAVP-treated apical membrane proteins were collected and mixed at a 1:1 ratio before analysis by LC-MS/MS using an LTQ-Orbitrap XL hybrid mass spectrometer. Mass spectrum acquisition and analysis are detailed in *SI Materials and Methods*.

Live-Cell Imaging. Cells were transfected with pLifeAct-TagGFP2, a plasmid encoding a GFP-conjugated 17-aa peptide that binds F-actin (but not G-actin) without interfering with F-actin dynamics (60). Transfected cells were grown on membrane supports until polarized before they were excised and mounted in a custom-made device for imaging (Fig. S4). Live-cell images were recorded using a confocal microscope LSM780 (Zeiss) equipped with a 37 °C chamber.

ACKNOWLEDGMENTS. We thank Suh-Yuen Liang (Core Facilities for Protein Structural Analysis, Academia Sinica) for assistance with protein MS. We thank Cheng-Yen Huang and Hua-Man Hsu (First Core Facility, National Taiwan University College of Medicine) for assistance with confocal and live-cell imaging. We thank Mathew Daniels and Patricia Connelly [Electron Microscope Core Facility, National Heart, Lung, and Blood

Institute (NHLBI)] for advice with immunoelectron microscopy. M.-J.Y. is supported by National Science Council, Taiwan Grants 100-2320-B-002-002-, 100-2320-B-002-097-, and 101-2320-B-002-038-MY3. M.A.K. is supported by the Intramural Budget of the NHLBI (Grant Z01-HL001285). R.A.F. is supported by the Danish Medical Research Council and the Lundbeck Foundation.

1. Knepper MA (2012) Systems biology in physiology: The vasopressin signaling network in kidney. *Am J Physiol Cell Physiol* 303(11):C1115–C1124.
2. Nielsen S, et al. (2002) Aquaporins in the kidney: From molecules to medicine. *Physiol Rev* 82(1):205–244.
3. Huling JC, et al. (2012) Gene expression databases for kidney epithelial cells. *Am J Physiol Renal Physiol* 302(4):F401–F407.
4. Yu MJ, et al. (2009) Systems-level analysis of cell-specific AQP2 gene expression in renal collecting duct. *Proc Natl Acad Sci USA* 106(7):2441–2446.
5. Pisitkun T, et al. (2006) High-throughput identification of IMCD proteins using LC-MS/MS. *Physiol Genomics* 25(2):263–276.
6. Uawithya P, Pisitkun T, Ruttenberg BE, Knepper MA (2008) Transcriptional profiling of native inner medullary collecting duct cells from rat kidney. *Physiol Genomics* 32(2):229–253.
7. Barile M, et al. (2005) Large scale protein identification in intracellular aquaporin-2 vesicles from renal inner medullary collecting duct. *Mol Cell Proteomics* 4(8):1095–1106.
8. Sachs AN, Pisitkun T, Hoffert JD, Yu MJ, Knepper MA (2008) LC-MS/MS analysis of differential centrifugation fractions from native inner medullary collecting duct of rat. *Am J Physiol Renal Physiol* 295(6):F1799–F1806.
9. Schenk LK, et al. (2012) Quantitative proteomics identifies vasopressin-responsive nuclear proteins in collecting duct cells. *J Am Soc Nephrol* 23(6):1008–1018.
10. Tchapyjnikov D, et al. (2010) Proteomic profiling of nuclei from native renal inner medullary collecting duct cells using LC-MS/MS. *Physiol Genomics* 40(3):167–183.
11. Yu MJ, et al. (2008) Large-scale quantitative LC-MS/MS analysis of detergent-resistant membrane proteins from rat renal collecting duct. *Am J Physiol Cell Physiol* 295(3):C661–C678.
12. Yu MJ, Pisitkun T, Wang G, Shen RF, Knepper MA (2006) LC-MS/MS analysis of apical and basolateral plasma membranes of rat renal collecting duct cells. *Mol Cell Proteomics* 5(11):2131–2145.
13. Tamma G, et al. (2011) Integrin signaling modulates AQP2 trafficking via Arg-Gly-Asp (RGD) motif. *Cell Physiol Biochem* 27(6):739–748.
14. Steffen A, et al. (2004) Sra-1 and Nap1 link Rac to actin assembly driving lamellipodia formation. *EMBO J* 23(4):749–759.
15. Rotty JD, Wu C, Bear JE (2013) New insights into the regulation and cellular functions of the ARP2/3 complex. *Nat Rev Mol Cell Biol* 14(1):7–12.
16. Ono S (2007) Mechanism of depolymerization and severing of actin filaments and its significance in cytoskeletal dynamics. *Int Rev Cytol* 258:1–82.
17. Lueck A, Brown D, Kwiatkowski DJ (1998) The actin-binding proteins adseverin and gelsolin are both highly expressed but differentially localized in kidney and intestine. *J Cell Sci* 111(Pt 24):3633–3643.
18. Noda Y, Horikawa S, Katayama Y, Sasaki S (2005) Identification of a multiprotein "motor" complex binding to water channel aquaporin-2. *Biochem Biophys Res Commun* 330(4):1041–1047.
19. Nurminsky D, Magee C, Faverman L, Nurminskaya M (2007) Regulation of chondrocyte differentiation by actin-severing protein adseverin. *Dev Biol* 302(2):427–437.
20. Cooper JA, Sept D (2008) New insights into mechanism and regulation of actin capping protein. *Int Rev Cell Mol Biol* 267:183–206.
21. Cao X, et al. (2005) PALS1 specifies the localization of ezrin to the apical membrane of gastric parietal cells. *J Biol Chem* 280(14):13584–13592.
22. Tamma G, et al. (2005) Actin remodeling requires ERM function to facilitate AQP2 apical targeting. *J Cell Sci* 118(Pt 16):3623–3630.
23. Ishikawa R, et al. (1994) Drebrin, a development-associated brain protein from rat embryo, causes the dissociation of tropomyosin from actin filaments. *J Biol Chem* 269(47):29928–29933.
24. Ishikawa R, et al. (2007) Drebrin attenuates the interaction between actin and myosin-V. *Biochem Biophys Res Commun* 359(2):398–401.
25. Nedvetsky PI, et al. (2007) A Role of myosin Vb and Rab11-FIP2 in the aquaporin-2 shuttle. *Traffic* 8(2):110–123.
26. Chew CS, Parente JA, Jr., Chen X, Chaponnier C, Cameron RS (2000) The LIM and SH3 domain-containing protein, lasp-1, may link the cAMP signaling pathway with dynamic membrane restructuring activities in ion transporting epithelia. *J Cell Sci* 113(Pt 11):2035–2045.
27. Michetti M, et al. (1996) Autolysis of human erythrocyte calpain produces two active enzyme forms with different cell localization. *FEBS Lett* 392(1):11–15.
28. Puliyanda DP, Ward DT, Baum MA, Hammond TG, Harris HW, Jr. (2003) Calpain-mediated AQP2 proteolysis in inner medullary collecting duct. *Biochem Biophys Res Commun* 303(1):52–58.
29. Tan I, Yong J, Dong JM, Lim L, Leung T (2008) A tripartite complex containing MRCK modulates lamellar actomyosin retrograde flow. *Cell* 135(1):123–136.
30. Moeller HB, Fenton RA (2012) Cell biology of vasopressin-regulated aquaporin-2 trafficking. *Pflugers Arch* 464(2):133–144.
31. Chou CL, et al. (2004) Non-muscle myosin II and myosin light chain kinase are downstream targets for vasopressin signaling in the renal collecting duct. *J Biol Chem* 279(47):49026–49035.
32. Taylor A, Mamelak M, Reaven E, Maffly R (1973) Vasopressin: Possible role of microtubules and microfilaments in its action. *Science* 181(4097):347–350.
33. Gao Y, Franki N, Macaluso F, Hays RM (1992) Vasopressin decreases immunogold labeling of apical actin in the toad bladder granular cell. *Am J Physiol* 263(4 Pt 1):C908–C912.
34. Ding GH, Franki N, Condeelis J, Hays RM (1991) Vasopressin depolymerizes F-actin in toad bladder epithelial cells. *Am J Physiol* 260(1 Pt 1):C9–C16.
35. Simon H, Gao Y, Franki N, Hays RM (1993) Vasopressin depolymerizes apical F-actin in rat inner medullary collecting duct. *Am J Physiol* 265(3 Pt 1):C757–C762.
36. Li W, et al. (2011) Simvastatin enhances aquaporin-2 surface expression and urinary concentration in vasopressin-deficient Brattleboro rats through modulation of Rho GTPase. *Am J Physiol Renal Physiol* 301(2):F309–F318.
37. Yui N, Lu HJ, Bouley R, Brown D (2012) AQP2 is necessary for vasopressin- and forskolin-mediated filamentous actin depolymerization in renal epithelial cells. *Biol Open* 1(2):101–108.
38. Klussmann E, et al. (2001) An inhibitory role of Rho in the vasopressin-mediated translocation of aquaporin-2 into cell membranes of renal principal cells. *J Biol Chem* 276(23):20451–20457.
39. Riethmüller C, et al. (2008) Translocation of aquaporin-containing vesicles to the plasma membrane is facilitated by actomyosin relaxation. *Biophys J* 94(2):671–678.
40. Noda Y, et al. (2004) Aquaporin-2 trafficking is regulated by PDZ-domain containing protein SPA-1. *FEBS Lett* 568(1-3):139–145.
41. Noda Y, et al. (2008) Reciprocal interaction with G-actin and tropomyosin is essential for aquaporin-2 trafficking. *J Cell Biol* 182(3):587–601.
42. Tamma G, et al. (2003) cAMP-induced AQP2 translocation is associated with RhoA inhibition through RhoA phosphorylation and interaction with RhoGDI. *J Cell Sci* 116(Pt 8):1519–1525.
43. Tamma G, et al. (2003) The prostaglandin E2 analogue sulprostone antagonizes vasopressin-induced antidiuresis through activation of Rho. *J Cell Sci* 116(Pt 16):3285–3294.
44. Sit ST, Manser E (2011) Rho GTPases and their role in organizing the actin cytoskeleton. *J Cell Sci* 124(Pt 5):679–683.
45. Tamma G, et al. (2001) Rho inhibits cAMP-induced translocation of aquaporin-2 into the apical membrane of renal cells. *Am J Physiol Renal Physiol* 281(6):F1092–F1101.
46. Schuster VL, Kokko JP, Jacobson HR (1984) Interactions of lysyl-bradykinin and antidiuretic hormone in the rabbit cortical collecting tubule. *J Clin Invest* 73(6):1659–1667.
47. Tamma G, Carmosino M, Svelto M, Valenti G (2005) Bradykinin signaling counteracts cAMP-elicited aquaporin 2 translocation in renal cells. *J Am Soc Nephrol* 16(10):2881–2889.
48. Noda Y, Sasaki S (2008) The role of actin remodeling in the trafficking of intracellular vesicles, transporters, and channels: Focusing on aquaporin-2. *Pflugers Arch* 456(4):737–745.
49. Duong Van Huyen J, Bens M, Vandewalle A (1998) Differential effects of aldosterone and vasopressin on chloride fluxes in transimmortalized mouse cortical collecting duct cells. *J Membr Biol* 164(1):79–90.
50. Nielsen S, et al. (1995) Vasopressin increases water permeability of kidney collecting duct by inducing translocation of aquaporin-CD water channels to plasma membrane. *Proc Natl Acad Sci USA* 92(4):1013–1017.
51. Khositseth S, et al. (2011) Quantitative protein and mRNA profiling shows selective post-transcriptional control of protein expression by vasopressin in kidney cells. *Mol Cell Proteomics* 10(1):M110.004036.
52. Rinschen MM, et al. (2010) Quantitative phosphoproteomic analysis reveals vasopressin V2-receptor-dependent signaling pathways in renal collecting duct cells. *Proc Natl Acad Sci USA* 107(8):3882–3887.
53. Hendriks G, et al. (2004) Glycosylation is important for cell surface expression of the water channel aquaporin-2 but is not essential for tetramerization in the endoplasmic reticulum. *J Biol Chem* 279(4):2975–2983.
54. Moeller HB, Praetorius J, Rützler MR, Fenton RA (2010) Phosphorylation of aquaporin-2 regulates its endocytosis and protein-protein interactions. *Proc Natl Acad Sci USA* 107(1):424–429.
55. Conti MA, Adelstein RS (2008) Nonmuscle myosin II moves in new directions. *J Cell Sci* 121(Pt 1):11–18.
56. Ebrahim S, et al. (2013) NMII forms a contractile transcellular sarcomeric network to regulate apical cell junctions and tissue geometry. *Curr Biol* 23(8):731–736.
57. Marazuela M, Alonso MA (2004) Expression of MAL and MAL2, two elements of the protein machinery for raft-mediated transport, in normal and neoplastic human tissue. *Histol Histopathol* 19(3):925–933.
58. Breton S, Brown D (1998) Cold-induced microtubule disruption and relocalization of membrane proteins in kidney epithelial cells. *J Am Soc Nephrol* 9(2):155–166.
59. Yui N, et al. (2013) Basolateral targeting and microtubule-dependent transcytosis of the aquaporin-2 water channel. *Am J Physiol Cell Physiol* 304(1):C38–C48.
60. Riedl J, et al. (2008) Lifeact: A versatile marker to visualize F-actin. *Nat Methods* 5(7):605–607.